[1]Kirti A. Patil

[2]R. P. Bhavsar

[3]B. V. Pawar

Optimized Deep Learning for Human age Estimation

JES Journal of Electrical Systems

Abstract: - Background/ Introduction: Human age assessment plays a crucial part in diagnosing genetic problems, and development abnormalities in children. They are also used in several applications, like forensic investigation and criminal scenes. Generally, human age is estimated from X-ray images of bones, and the manual estimation of human age is highly subjective, as they depend on the medical experience of the professionals. Further, they are prone to error and are laborious, thereby requiring automated Bone Age Assessment (BAA) for determining human age with high accurateness.

Materials and methods: This work presents a novel approach using Deep Learning (DL) and optimization considering the X-ray images of hand. Here, human age is estimated using the Deep Residual Network (DRN), whose parameters are trained using the proposed Beluga whale lion optimization (BWLO) algorithm. Further, several processes, like pre-processing, Region of Interest (RoI) extraction, Image augmentation, and feature extraction are used to enhance the accuracy of the estimation model.

Results and conclusion: The BWLO_DRN is examined for its superiority considering metrics, like accuracy, Sensitivity, Specificity, Positive Predictive Value (PPV) and Negative Predictive Value (NPV).

Keywords: image processing, neural network, optimization, forensic investigation, bone age

I. BACKGROUND

The chronological age and biological age are the two main "ages" used in the medical field to gauge human growth and development. The birth date determines the age of chronology, which is one of them. The biological age mostly indicates how humans have evolved, which is primarily based on the teeth and bone age. [1]. The use of appropriate methods for the age determination is necessary in medico-legal contexts. Skeletal age assessment (SAA) and understanding of growth steps have an essential role in regular practice of paediatrician as well as of endocrinologist [2,3]. Bones vary significantly in shape over the course of a lifetime. Bone age is a continual measurement of the level of actual bone formation [4]. Bones represents strong changes during development. The arm consists of 8 carpals, 5 metacarpals, and 14 phalanges in addition with radius and ulna, so there are 29 in total. The hand is a perfect body component for taking X-ray images because of the high bone density in a relatively limited spatial volume [5]. The most common method for detecting SAA involves comparing radiographs of the left hand (non-dominant) hand and wrist with hand-wrist atlases of children of the same gender and age [4]. According to estimates, 76% of radiologists determine the bone age of patients by quickly and easily comparing left hand X-ray pictures with a reference atlas. However, this approach is sensitive, based on experience, and variable between observers, meaning that the accuracy of bone age assessment (BAA) depends on the expertise of medical professionals [6]. BAA is a tool used by clinicians to gauge a child's skeletal system's maturity. BAA procedures often begin with a single X-ray scan of the left hand from the wrist to the fingertips, [2,3]. Bone age is a measurement of a child's growth and development at a specific age. The difference between bone age and chronological age is strongly

correlated with physical maturation, including body size, the emergence of sex character changes, pubertal growth spurt, and endocrine hormone levels. It exhibits a perfectly consistent link with the body's physical development and is the most accurate marker for gauging personal development. For the research of endocrine, genetic, and

1MET's Institute of Engineering, BKC, Nashik, India

kirti.patil2004@gmail.com

[2]School of Computer Sciences, NMU, Jalgaon, India

rpbhavsar@nmu.ac.in

[3]KCES's Institute of Management & Research, Jalgaon (MS), India

bvpawar@imr.ac.in

* Corresponding Author Email:Kirti.patil2004 @email.com

development issues in teenagers, BAA is a widely utilized clinical technique [7, 8]. Radiologists perform BAA in clinical settings by looking at a left-hand wrist X-ray picture [9] where deep learning technique finds increasing use cases in diverse medical information processing and analysis fields. Deep Learning-based bone age estimation methods have developed rapidly and have achieved significant improvements compared to conventional methods [10]. With the rapid development of computer vision and medical image analysis and processing, deep learning methods, which can model input data and approach complex tasks through deep linear networks, have the ability to extract excellent automatic features that are very useful in the medical field. The high-resolution carpal and meta-carpal bone regions were used instead of the entire hand region for bone age

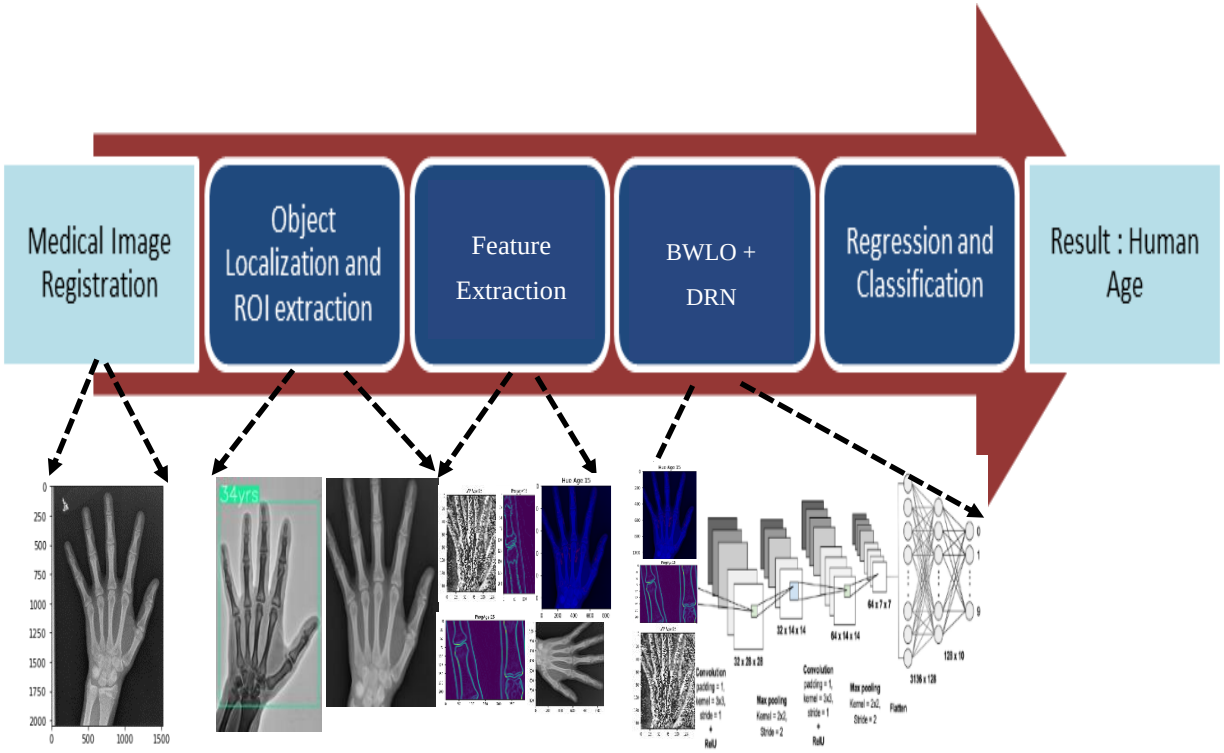

Figure 1: An Automated Model

estimate in the attention guided technique, which localized the discriminative regions using image level labels. [11]. The benefits of a Global-Local feature fusion with CNN approach include quick diagnostic times, labour savings, and significantly less work for the doctor with highly reproducibleresults [12] whereas this method was failed to consider the interpretability of deep learning for achieving more accurate estimation. Using MRI and X-ray images, the deep learning-based models successfully fixed issues with automatic segmentation, classification, and prediction. For image identification, segmentation, prediction, and classification utilizing MRI and X-ray images, powerful deep-learning models include the convolutional neural network (CNN), deep belief network (DBN), and deep residual network (DRN) [13].

II. MATERIALS AND METHODS

This research aims to design and develop a optimized deep learning for human age estimation using hand X-ray images. The first step for estimating the age is pre-processing. Here, the input hand X-ray image is pre-processed using the Non-Local Means filter (NLMF) [14]. After that, the ROI extraction process is carried out. Then, the image is augmented by considering various processes, like scaling, cropping, rotation, translation, and flipping, and the color augmentation, such as brightness, contrast, saturation, and Hue. After image augmentation, the feature extraction process is done, where the CNN features, statistical features, Gray Level Co-occurrence matrix (GLCM) texture features [15,16], Local Vector Pattern (LVP)features [15], Pyramid Histogram of Oriented Gradients (PhoG) feature [18], Complete Local Binary Pattern (CLBP) features [19] are extracted. The final step is hand bone age estimation, which is done by Deep Residual Network (DRN) [20]. The DRN is trained with proposed Beluga whale lion optimization (BWLO). The BWLO will be designed by integrating the Beluga whale optimization (BWO)[21], and Sea Lion Optimization (SLO)[22]. Thus, the human bone age is estimated by the optimized DL approach using

hand X-ray image. In addition, the metrics, like Accuracy, Positive Predictive Value (PPV), and Negative Predictive Value (NPV), Sensitivity, Specificity and the comparative analysis will be done with proposed and existing methods [5][10][11] and [12] to reveal the effectiveness of the proposed system. Figure 1 depicts the block diagram of human age estimation using hand X-ray image.

2.1 Dataset Description and Experimental Setup

The hand-Xray digital images are collected from the RSNA Bone Age Detection [23]. It consists of hand X-ray images of children, which are utilized in accurate determination of the child's age. It consists of numerous digital and scanned images with a CSV file comprising of the gender and the child's age to be estimated. The real-time dataset digital images are collected with and without labels from clinics and hospitals. A total of 500 images are present in the dataset with labels and 174 images without labels, and in this work, only images with labels are considered. Due to data privacy issues, gender data is not included in this study, which aims to develop a reliable assessment procedure that is gender neutral. This model is implemented on the Python platform with Keras front-end and Tensorflow back-end, parallelized with NVIDIA GEFORCE GTX 1050 graphics processing unit (GPU).

2.2. EXPERIMENTAL RESULTS

In this segment, the image analysis of the BWLO_DRN for hand bone age estimation is carried out, and is represented in figure 2.

Figure 2a) represents the input image obtained from the RSNA Bone Age Detection dataset, the corresponding pre-processed and RoI images are displayed in figure 2b), and figure 2c). The images obtained as a result of various augmentation techniques are represented by figure 2d) for brightness, figure 2e) for contrast, figure 2f) for cropping, figure 2g) for flipping, figure 2h) for hue, figure 2i) for rotation, figure 2j) for saturation, figure 2k) for scaling, and figure 2l) for translation correspondingly. Figure 2m) indicates CLBP feature extracted image, figure 2n), and figure 2o) indicate the LVP, and PHoG feature images.

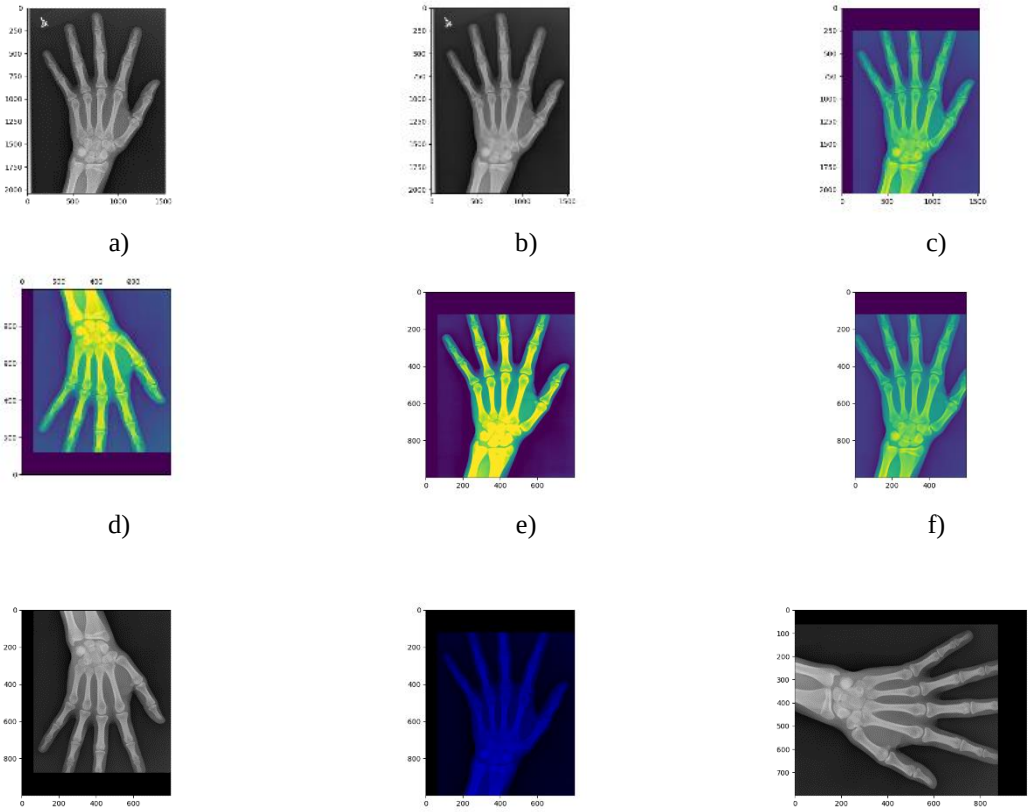

a) b) c)

d) e) f)

g) h) i)

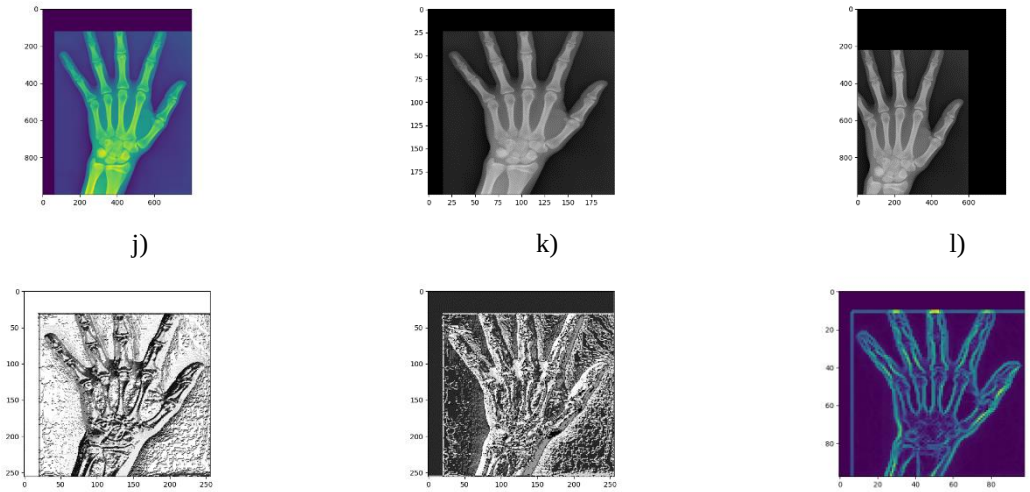

j) k) l)

m) n) o)

Figure 2: Experimental outcomes of the BWLO_DRN for bone age estimation with a) input, b) pre-processed, c) RoI, d) brightness augmented, e) contrast augmented, f) cropped, g) flipped, h) hue augmented, i) rotated, j) saturated, k) scaled, l) translated, m) CLBP, n) LVP, and o) PHoG images

2.3. COMPARATIVE TECHNIQUES

The BWLO_DRN proposed in this work for estimating bone age using the hand X-ray images is investigated for its effectiveness by comparing it with techniques, such as DL [1], MLP [3], Global_local feature_CNN [4], and Attention-guided approach [6] by considering the images obtained from RSNA Bone Age Detection and a real-time dataset.

2.4. COMPARATIVE ASSESSMENT

The comparative analysis of the BWLO_DRN presented in this work for estimating bone age using the hand X-ray images is carried out using the images acquired from the dataset-1 and real-time dataset based on different metrics, like accuracy, sensitivity, specificity, PPV, and NPV.

2.4.1. Using RSNA Bone Age Detection Dataset

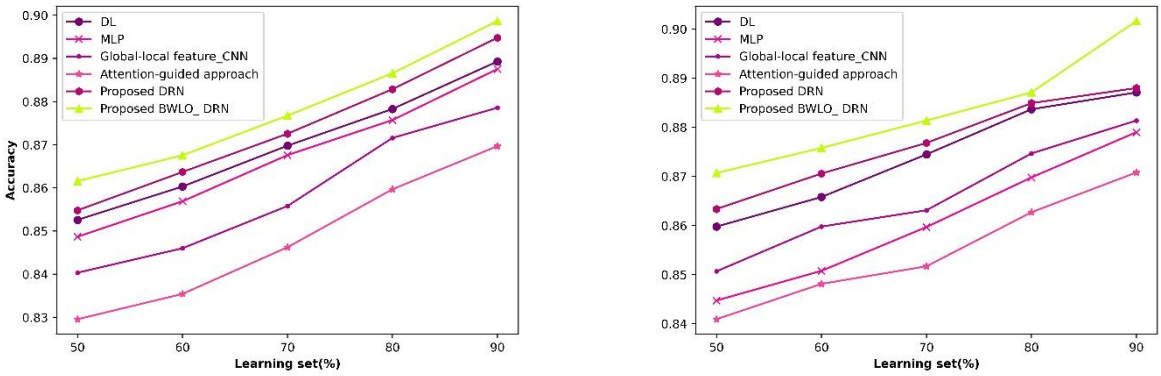

a) b)

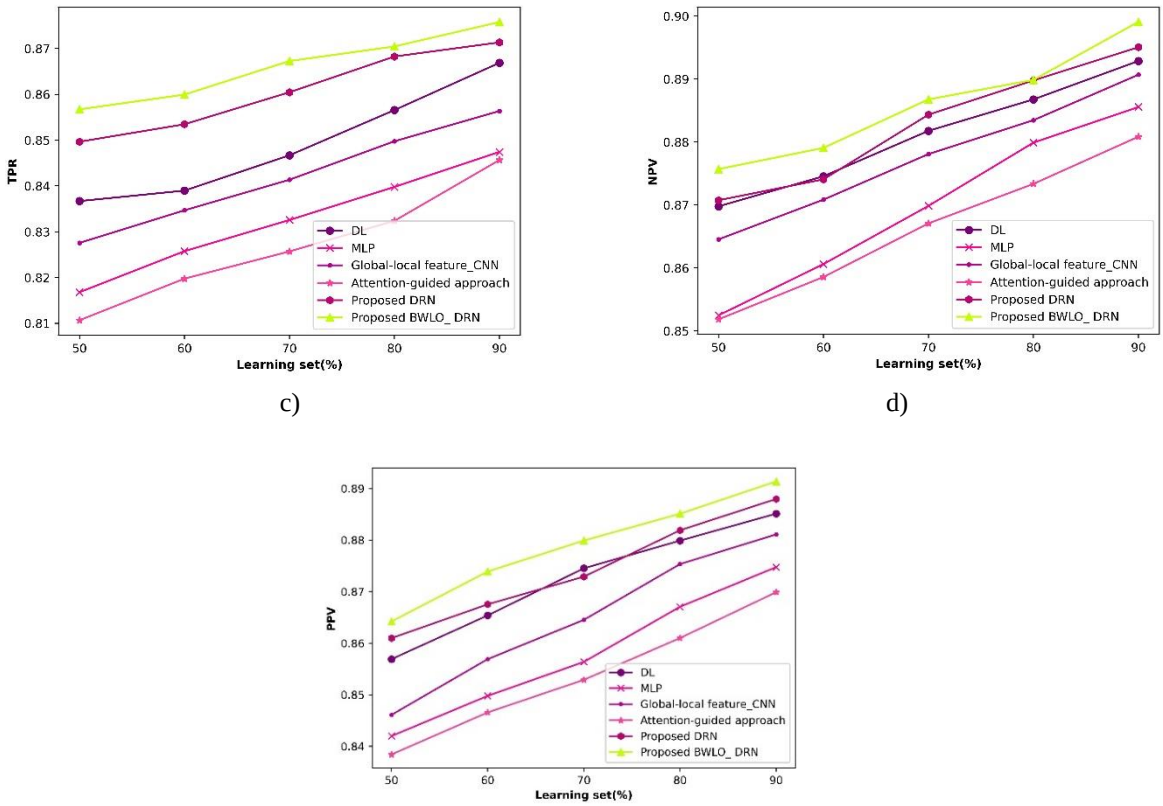

c) d)

e)

Figure 3: Comparative analysis of the BWLO_DRN in view of a) Accuracy, b) Specificity, and c) Sensitivity, d) NPV, and e) PPV using RSNA Bone Age Detection dataset

Figure 3, portrays the comparative valuation of the BWLO_DRN considering images acquired from RSNA Bone Age Detection dataset. The assessment of the BWLO_DRN on the basis of accuracy is displayed in figure 3a). With a learning set of 50%, the BWLO_DRN attained an accuracy of 0.860, while the BAA techniques, such as DL, MLP, Global-local feature CNN, and Attention-guided approach measured the accuracies of 0.851, 0.846, 0.839, and 0.826. This shows that the BWLO_DRN realized an improved performance of 1.07%, 1.62%, 2.36%, and 3.97%. Figure 3b) displays the investigation of the BWLO_DRN using specificity.

Thus, the BWLO_DRN is found to succeed in producing a higher variation in specificity by 1.03%, 2.73%, 1.92%, and 3.22%. at 60% learning set. The BWLO_DRN is effective in producing a higher performance enhancement of 1.03%, 3.16%, 1.96%, and 3.58% with 70% learning set. Similarly, the evaluation of the BWLO_DRN considering NPV is demonstrated using figure 3d). The BWLO_DRN attained an NPV of 0.879, with 60% learning set, and computed NPV values of 0.873, 0.859, 0.868, and 0.856 with respect to DL, MLP, Global_local feature_CNN, and Attention-guided approach. This discloses that the BWLO_DRN attained a high performance of 0.65%, 2.33%, 1.25%, and 2.66% respectively. The examination of the BWLO_DRN on the basis of PPV is exhibited in figure 3e).

Dataset	***Metrics***	***DL***	***MLP***	***GLF-CNN***	***AGA***	***Proposed BWLO_DRN***
RSNA Bone Age Detection [EffnetB4] TF dataset	***Accuracy***	0.893	0.895	0.878	0.869	0.898
	Sensitivity	0.866	0.847	0.856	0.843	0.875
	Specificity	0.887	0.878	0.881	0.870	0.901
	NPV	0.893	0.885	0.890	0.880	0.899
	PPV	0.885	0.875	0.881	0.870	0.891
Real-time dataset	***Accuracy***	0.888	0.881	0.886	0.879	0.894

	Sensitivity	0.857	0.861	0.851	0.847	0.871
	Specificity	0.884	0.878	0.869	0.864	0.891
	NPV	0.877	0.874	0.887	0.886	0.895
	PPV	0.883	0.862	0.875	0.877	0.887

*Deep Learning (DL), Multi-Layer Perceptron (MLP), Global-Local Feature fusion Convolutional Neural Network (GLF-CNN), Attention-Guided Approach (AGA), Radiological Society of North America (RSNA), Positive Predictive Value (PPV), Negative Predictive Value (NPV).

With 50% learning set, the PPV measured by DL, MLP, Global_local feature_CNN, Attention-guided approach and BWLO_DRN is 0.857, 0.842, 0.846, 0.838, and 0.864. Thus, the BWLO_DRN is found to attained a performance improvement of 0.85%, 2.57%, 2.09%, and 2.98%.

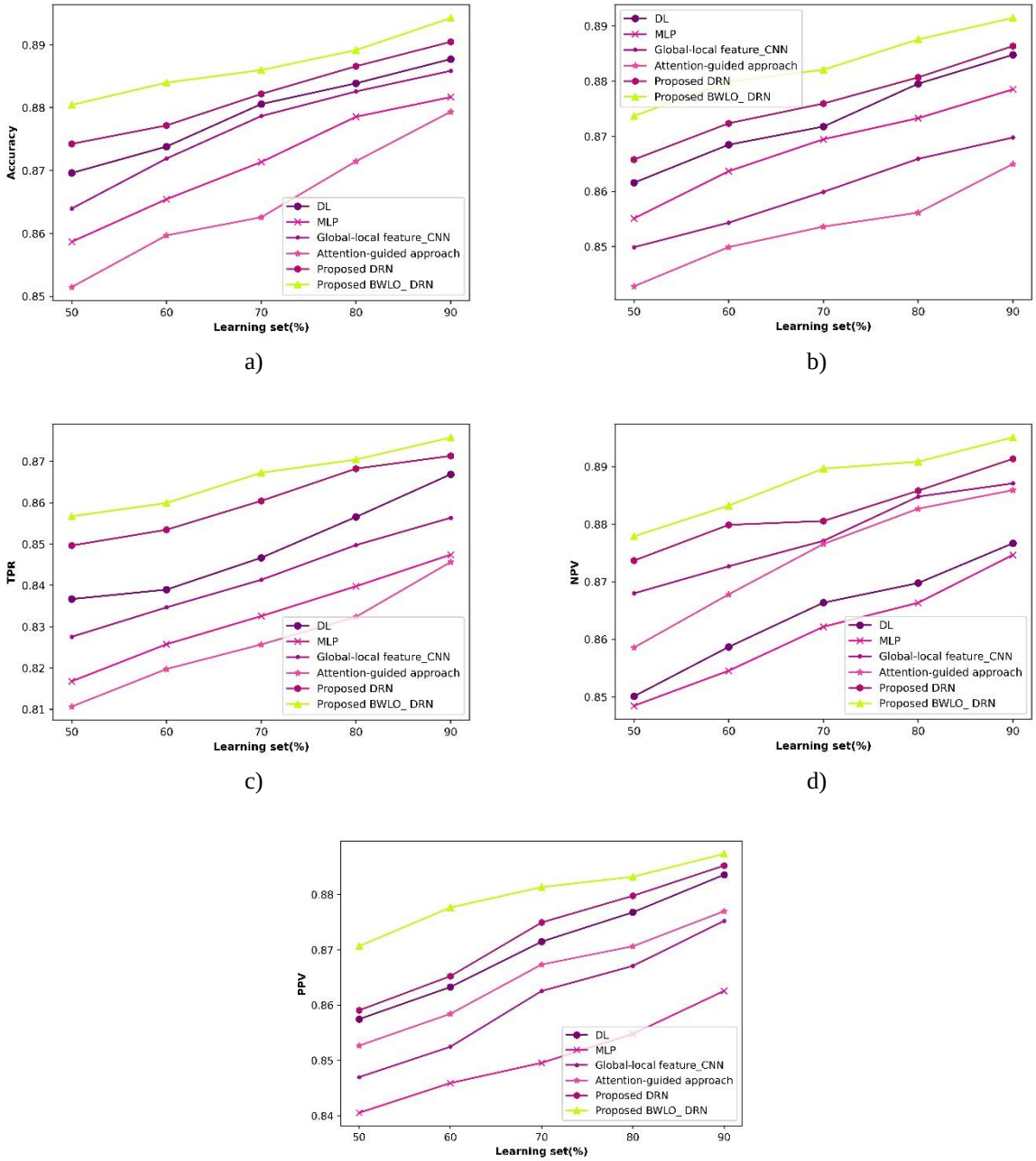

Figure 4: Comparative evaluation of the BWLO_DRN with respect to a) Accuracy, b) Specificity, and c) Sensitivity, d) NPV, and e) PPV using real-time dataset

2.4.2. With real-time dataset

The comparative evaluation of the BWLO_DRN based on the X-ray images acquired from real-time dataset is presented in figure 3. The accuracy-based examination of the BWLO_DRN is shown in figure 4a). The accuracy attained by BWLO_DRN is 0.884, while the other BAA approaches attained accuracy of 0.880, 0.866, 0.876, and 0.860 for DL, MLP, Global_local feature_CNN, and Attention-guided approach respectively, with 70% learning set. This depicts that BWLO_DRN achieved a performance improvement of 0.44%, 2.04%, 0.90%, and 2.72%. Figure 4b) illustrates the comparative assessment of the BWLO_DRN in view of specificity. Specificity computed by DL, MLP, Global_local feature_CNN, Attention-guided approach and BWLO_DRN is 0.884, 0.873, 0.866, 0.860, and 0.890, with 80% learning set. This displays that the BWLO_DRN is effectual in producing a higher performance enhancement of 0.61%, 1.84%, 2.67%, and 3.36%. The valuation of the BWLO_DRN concerning sensitivity is displayed in figure 4c) for 70% learning set, the BWLO_DRN achieved a sensitivity of 0.860, while the BAA techniques, like DL, MLP, Global_local feature_CNN, and Attention-guided approach attained sensitivity of 0.846, 0.849, 0.840, and 0.830. This illustrates that the BWLO_DRN realized an enhanced performance of 1.65%, 1.29%, 2.34%, and 3.49%. Figure 4d) displays the analysis of the BWLO_DRN based on NPV. With 60% learning set, the NPV values realized by DL is 0.859, MLP is 0.855, Global_local feature_CNN is 0.873, Attention-guided approach is 0.863, and the BWLO_DRN is 0.883. This reveals that the BWLO_DRN attained a higher performance improvement of 2.74%, 3.20%, 1.13%, and 2.23%. The PPV-based analysis of the BWLO_DRN is displayed in figure 4e). The BWLO_DRN calculated a PPV of 0.873, with 60% learning set, while the methods, like DL, MLP, Global_local feature_CNN, and Attention-guided approach computed PPV values of 0.865, 0.841, 0.851, and 0.857. This illustrates that the BWLO_DRN realized an enhanced performance of 0.83%, 3.59%, 2.49%, and 1.85%.

III. CONCLUSION

In this work, an efficient human age estimation approach is developed, wherein Deep Learning (DL) approaches are utilized for estimating the bone age from the X-ray images of the hand. Here, human bone age is determined using the Deep Residual Network (DRN), based on the most significant features of the input X-ray image. Further, the efficiency of the DRN in estimating bone age is enhanced by the utilization of the Beluga whale lion optimization (BWLO) algorithm for training the DRN. Further, the BWLO_DRN is examined for its superiority considering metrics, like accuracy, Positive Predictive Value (PPV), Negative Predictive Value (NPV), Sensitivity, and Specificity, and the experimentation reveals that the BWLO_DRN is effective in attaining superior value of accuracy at 0.894, PPV at 0.887, NPV at 0.895, sensitivity at 0.871, and specificity of 0.891, thus producing exceptional performance.

In future, multiple body parts can be considered to estimate the accurate human age, provided that the large number of medical images and its relevant data is available.

REFERENCES

[1] Han, Y. and Wang, G., “Skeletal bone age prediction based on a deep residual network with spatial transformer”, Computer Methods and Programs in Biomedicine, vol. 197, pp.105754, 2020.

[2] K. A. Patil, R. P. Bhavsar, and B. V. Pawar, “Features and methods of human age estimation: Opportunities and challenges in medical image processing”, Turkish Journal of Computer and Mathematics Education (TURCOMAT), 2021, Vol. 12, Issue 1S, 294-318.

[3] De Sanctis, V., Di Maio, S., Soliman, A.T., Raiola, G., Elalaily, R. and Millimaggi, G., “Hand X-ray in pediatric endocrinology: Skeletal age assessment and beyond.” Indian journal of endocrinology and metabolism, vol.18 (Suppl 1), pp.S63, 2014.

[4] Zulkifley, M.A., Mohamed, N.A., Abdani, S.R., Kamari, N.A.M., Moubark, A.M. and Ibrahim, A.A., “Intelligent bone age assessment: an automated system to detect a bone growth problem using convolutional neural networks with attention mechanism”, Diagnostics, vol.11, no.5, pp.765, 2021.

[5] Lee, J.H., Kim, Y.J. and Kim, K.G., “Bone age estimation using deep learning and hand X-ray images”, Biomedical Engineering Letters, vol.10, no.3, pp.323-331, 2020.

[6] Guo, J., Zhu, J., Du, H. and Qiu, B., “A bone age assessment system for real-world X-ray images based on convolutional neural networks”, Computers & Electrical Engineering, vol.81, pp.106529, 2020.

[7] Lee H, Tajmir S, Lee J, Zissen M, Yeshiwas BA, Alkasab TK, Choy G, Do S (2017) “Fully automated deep learning system for bone age assessment.”, J Digit Imaging, 30:427–441. https://doi.org/10.1007/s10278-017-9955-8.

[8] Patil, K. A. ., R. P. Bhavsar, & B. V. Pawar. (2023). A Multi-featured Approach by Integrating Digital Hand and Dental X-Ray for Human Age Estimation. Journal of Advanced Zoology, 44(S3), 1144–1148. https://doi.org/10.17762/jaz.v44iS-3.1204

[9] Gao, Y., Zhu, T. and Xu, X., "Bone age assessment based on deep convolution neural network incorporated with segmentation", International Journal of Computer Assisted Radiology and Surgery, vol.15, no.12, pp.1951-1962, 2020.

[10] Li, S., Liu, B., Li, S., Zhu, X., Yan, Y. and Zhang, D., "A deep learning-based computer-aided diagnosis method of X-ray images for bone age assessment", Complex & Intelligent Systems, vol.8, no.3, pp.1929-1939, 2022.

[11] Chen, C., Chen, Z., Jin, X., Li, L., Speier, W. and Arnold, C.W., "Attention-guided discriminative region localization and label distribution learning for bone age assessment", IEEE Journal of Biomedical and Health Informatics, vol.26, no.3, pp.1208-1218, 2021.

[12] Hui, Q., Wang, C., Weng, J., Chen, M. and Kong, D., "A Global-Local Feature Fusion Convolutional Neural Network for Bone Age Assessment of Hand X-ray Images", Applied Sciences, vol.12, no.14, p.7218, 2022.

[13] Nadeem, M.W., Goh, H.G., Ali, A., Hussain, M., Khan, M.A. and Ponnusamy, V.A.P., "Bone age assessment empowered with deep learning: a survey, pen research challenges and future directions", Diagnostics, vol.10, no.10, pp.781, 2020.

[14] Wang, G., Liu, Y., Xiong, W. and Li, Y., "An improved non-local means filter for colour image denoising", Optik, vol.173, pp.157-173, 2018.

[15] Chen, X., Li, J., Zhang, Y., Lu, Y. and Liu, S., "Automatic feature extraction in X-ray image based on deep learning approach for determination of bone age" Future Generation Computer Systems, vol.110, pp.795-801, 2020.

[16] Chilakala, L.R. and Kishore, G.N., "Optimal deep belief network with opposition-based hybrid grasshopper and honeybee optimization algorithm for lung cancer classification: A DBNGHHB approach", International Journal of Imaging Systems and Technology, vol.31, no.3, pp.1404-1423, 2021.

[17] Fan, K.C. and Hung, T.Y., "A novel local pattern descriptor—local vector pattern in high-order derivative space for face recognition", IEEE transactions on image processing, vol.23, no.7, pp.2877-2891, 2014.

[18] Bai, Y., Guo, L., Jin, L. and Huang, Q., "A novel feature extraction method using pyramid histogram of orientation gradients for smile recognition", In proceedings of 2009 16th IEEE International Conference on Image Processing (ICIP), pp. 3305-3308, 2009.

[19] Ahmed, F., Bari, H. and Hossain, E., "Person-independent facial expression recognition based on compound local binary pattern (CLBP)", Int. Arab J. Inf. Technol., vol.11, no.2, pp.195-203, 2014.

[20] Chen, Z., Chen, Y., Wu, L., Cheng, S. and Lin, P., "Deep reidual network-based fault detection and diagnosis of photovoltaic arrays using current-voltage curves and ambient conditions", Energy Conversion and Management, vol.198, p.111793, 2019.

[21] Zhong, C., Li, G. and Meng, Z., "Beluga whale optimization: A novel nature-inspired metaheuristic algorithm", Knowledge-Based Systems, pp.109215, 2022.

[22] Masadeh, R., Mahafzah, B.A. and Sharieh, A., "Sea lion optimization algorithm", International Journal of Advanced Computer Science and Applications, vol.10, no.5, 2019.

[23] RSNA Bone Age Detection [EffnetB4] TF dataset take from "https://www.kaggle.com/code/muki2003/rsna-bone-age-detection-effnetb4-tf/data", accessed on December 2022.